J. Marine Sci. Appl. (2010) 9: 445-450
DOI: 10.1007/s11804-010-1032-3

Phase Difference Method for DOA Estimation

Zhi-fei Chen*, Jin-cai Sun and Hong Hou

College of Marine, Northwestern Polytechnical University, Xi'an 710072, China

Abstract: The phase difference method (PDM) is presented for the direction of arrival (DOA) estimation of the narrowband source. It estimates the DOA by measuring the reciprocal of the phase range of the sensor output spectra at the interest frequency bin. The peak width and variance of the PDM are presented. The PDM can distinguish closely spaced sources with different and unknown center frequencies as long as they are separated with at least one frequency bin. The simulation results show that the PDM has a better resolution than that of the conventional beamforming.
Keywords: direction of arrival(DOA); phase difference; peak width; variance; resolution
Article ID: 1671-9433(2010)04-0445-06

1 Introduction

The phase difference is widely used in the time delay estimation, the phase comparison (PC) method and the sinusoidal frequency estimation. Regarding the phase difference information is preserved after computing the cross correlation function between two sensor samples, the generalized cross correlation (GCC) method (Carter, 1987) constructs a framework for the time delay estimation. However, the choice of the weight function has a great effect on the performance of the GCC method.

The PC method is widely applied in the monopulse radar and the phase interferometer (Bird *et al.*, 2005; Lurton X, 2000). Since the array configuration is available, the incoming azimuth could be extracted directly from the measured phase difference in the PC method. It shows us a compact method on the DOA estimation problem with high accuracy and low computation load without angle scanning. However, the measured phase is limited in (-π, π]. Therefore, the baseline length of the phase interferometer determines the available frequency range and angle resolution. A short baseline indicates a large frequency range and a low angle resolution (Shieh *et al*., 2000). To balance the frequency range and the angle resolution, the phase interferometer always has multiple baselines whose geometry is also carefully designed according to different applications, *e.g.* very long baseline interferometry (Hobiger *et al*., 2009).

In the field of sinusoidal frequency estimation, Kay first presented a method utilizing the weighted average of the phase difference (Fowler, 2002; Kay, 1989). It avoids the problem of phase ambiguity. Then many improved methods are introduced. Most of them take a preprocessing step, *e.g.* autocorrelation (Xiao *et al*., 2007), cross correlation (Umesh *et al*., 1996) and filter (Daeyoung *et al*., 1996), to improve the signal to noise ratio (SNR). The phase difference among the different segments of the recorded data after the Fast Fourier Transform algorithm method (FFT) is also applied to estimate the sinusoidal frequency (Jin, 2008). In essence, these methods are similar to the PC method (Fowler *et al*., 1999).

Different from the methods above, we introduce a DOA estimation method with the process of searching the phase difference. Note that the signal phase angles will be equal to each other when the searching angle aims at the true azimuth in the conventional beamforming method (CBF). Then the phase difference between the maximum and minimum phases of the spectra at the center frequency bin tends to zero. If we take the reciprocal of the phase difference as an estimator, it shows us a peak at the true azimuth. It is denoted as the phase difference method (PDM). Its peak width and variance on the DOA estimation is presented. The PDM could distinguish closely spaced sources with different and unknown center frequencies.

2 Phase difference method

Consider a uniform linear array (ULA) with M elements receiving a narrowband source emitted from θ_0 whose visible region is [-π/2, π/2]. The sensor displacement $d \le \lambda/2$, where λ denotes the wavelength of the corresponding frequency bin ω_0. The M×1 complex vector of array observation $\boldsymbol{x}$ with K snapshots can be modeled as

$$\boldsymbol{x}(k) = \boldsymbol{A}s(k) + \boldsymbol{n}(k),\ k=1,\ldots,\ K \qquad (1)$$

where $\boldsymbol{A} = \left[1, \mathrm{e}^{-\mathrm{j}\omega_0\tau_0}, \ldots, \mathrm{e}^{-\mathrm{j}(M-1)\omega_0\tau_0}\right]^{\mathrm{T}}$ denotes the array manifold. Here, T represents the matrix transpose and $\tau_0 = (d\sin\theta_0)/c$, where c is the wave speed in the propagation medium. $s(k)$ is the signal and $\boldsymbol{n}(k)$ is the

Received date: 2009-12-31.
Foundation item: Supported by the National Science Foundation under Grant No. 60672136 and the the Doctorate Foundation of Northwestern Polytechnical University under Grant No. CX200803.
***Corresponding author Email:** chenzhifei@gmail.com

white Gaussian noise with zero mean and σ^2 variance. When the propagation parameters and ω_0 are available, the steering vector only depends on the DOA to be estimated.

In the frequency domain, the sensor output spectrum at ω_0 is

$$\boldsymbol{X}(\omega_0)=\boldsymbol{A}S_0(\omega_0)+\boldsymbol{N}(\omega_0) \tag{2}$$

where $\boldsymbol{X}(\omega_0)$ and $\boldsymbol{N}(\omega_0)$ represent the array output spectrum vector and the noise spectrum vector at ω_0, respectively. $S_0(\omega_0)$ denotes the spectrum of $s(k)$ at ω_0. For simplicity, the signs ω_0 will be omitted. After phase compensation with $\mathbf{w}=\left[1,\mathrm{e}^{-\mathrm{j}\omega_0\tau},...,\mathrm{e}^{-\mathrm{j}(M-1)\omega_0\tau}\right]^{\mathrm{T}}$ on both sides of Eq.(2), where $\tau=(d\sin\theta)/c$ and θ denotes the searching angle, we get

$$\boldsymbol{X}'=\boldsymbol{w}^*\odot[\boldsymbol{A}S_0]+\boldsymbol{N}' \tag{3}$$

where $\boldsymbol{X}'=\boldsymbol{w}^*\odot\boldsymbol{X}$, $\boldsymbol{N}'=\boldsymbol{w}^*\odot\boldsymbol{N}'$. Here, the superscript $*$ denotes the conjugate and $\odot$ is the Hadamard product. It is the same with the phase compensation of the CBF method in the frequency domain. Let $S_0=A\mathrm{e}^{j\alpha}$, where A and α are the amplitude and phase of S_0, respectively. Both of them are unknown but constant. Rewriting the mth element of $\boldsymbol{X}'$, we find

$$X_m'=A\mathrm{e}^{\mathrm{j}[\alpha+(m-1)\omega_0(\tau-\tau_0)]}+N_m'=B_m\mathrm{e}^{\mathrm{j}[\alpha+(m-1)\omega_0(\tau-\tau_0)+\beta_m]} \tag{4}$$

where B_m is the amplitude of X_m' and β_m is the phase interference caused by the noise spectrum N_m'. Consequently, $\boldsymbol{B}=[B_1,...,B_M]^{\mathrm{T}}$ and $\boldsymbol{\beta}=[\beta_1,...,\beta_M]^{\mathrm{T}}$ are the amplitude vector and the phase interference vector of $\boldsymbol{X}'$. They are random variables with respect to θ. Then the measured phase of X_m' is

$$\varphi_m(\theta)=\alpha+(m-1)\omega_0(\tau-\tau_0)+\beta_m \mod 2\pi \tag{5}$$

where mod means an appropriate choice of addition with 2π interval to make φ_m lie in $(-\pi,\pi]$. Then the phase difference $\psi(\theta)$ between the maximum and minimum phases of $\boldsymbol{X}'$ becomes

$$\psi(\theta)=\max[\boldsymbol{\varphi}(\theta)]-\min[\boldsymbol{\varphi}(\theta)]=\mathrm{range}[\boldsymbol{\varphi}(\theta)] \tag{6}$$

where $\boldsymbol{\varphi}(\theta)=[\varphi_1,...,\varphi_M]^{\mathrm{T}}$ is the measured phase vector of $\boldsymbol{X}'$. The operation *range* denotes the phase difference computation defined in Eq.(6). Then we take the reciprocal of the phase difference after phase compensation as the estimator of the phase difference method (PDM). It follows that

$$P_{PDM}(\theta)=\frac{1}{\psi(\theta)} \tag{7}$$

which provides the PDM spectrum for the bearing estimation.

3 Performance analysis

3.1 Peak width

The peak width of the PDM is defined as the 3dB angle distance of the peak of the PDM spectrum after normalization in dB form as shown in Fig.1. At moderate and high SNRs, we get the measured phases $\alpha+(m-1)\omega_0(\tau-\tau_0)+\beta_m$ without the mod computation when θ is around θ_0, which is plotted in Fig.2. Then the maximum and the minimum phases belong to the Mth and the first elements of $\boldsymbol{\varphi}(\theta)$ in general. It implies that $\left|\alpha+(M-1)\omega_0(\tau-\tau_0)\right|\le\pi$. Expanding it, we have

$$\arcsin\left[\frac{-\lambda(\pi+\alpha)}{(M-1)2\pi d}+\sin\theta_0\right]\le\theta\le\arcsin\left[\frac{\lambda(\pi-\alpha)}{(M-1)2\pi d}+\sin\theta_0\right] \tag{8}$$

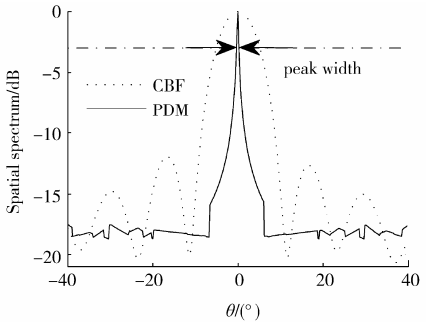

Fig.1 Spatial spectra when θ_0=0°, M=10, SNR=10dB

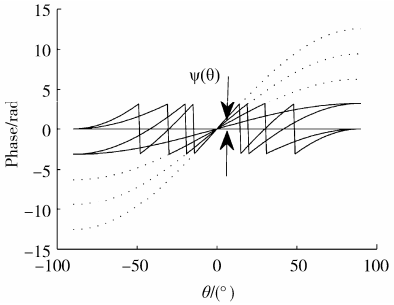

Fig.2 Phase curves of $\varphi(\theta)$ without phase interference when θ_0=0°, M=5, α=0; the solid lines denote the measured phases $\varphi_m(\theta)$, and the dashed lines are the corresponding phase curves without mod computation.

In the condition of inequality (8), the phase difference is close to

$$\psi(\theta)\approx\left|(M-1)\frac{2\pi d}{\lambda}(\sin\theta-\sin\theta_0)+\beta_M-\beta_1\right| \tag{9}$$

Defining $\hat{\theta}$ as the estimate of θ_0. Then $\psi(\hat{\theta}) \approx \text{range}(\boldsymbol{\beta})$ tends to the minimum phase difference in the process of searching angle. At the right 3dB point θ_h, we have

$$\psi(\theta_h) \approx (M-1)\frac{2\pi d}{\lambda}\left(\sin\theta_h - \sin\hat{\theta}\right) + \beta_M - \beta_1 = 2\text{range}(\boldsymbol{\beta})$$

Here, $(\beta_M - \beta_1)$ asymptotically follows the Gaussian distribution $N(0, \rho^{-1})$ (see Appendix A), where $\rho = A_0^2/(2\sigma^2)$ represents the SNR. $A_0 = \sqrt{2A^2/K}$ is the corresponding amplitude of S_0 in the time domain. Since $(\beta_M - \beta_1)$ approaches to zero in a large probability at moderate and high SNRs, we take $(\beta_M - \beta_1) \approx 0$. It follows that

$$\theta_h = \arcsin\left(\frac{\lambda\text{range}(\boldsymbol{\beta})}{(M-1)\pi d} + \sin\hat{\theta}\right)$$

Consequently, the peak width of the PDM is

$$\text{PW}_{\text{PDM}} = 2\left|\theta_h - \hat{\theta}\right| \approx 2\left|\arcsin\left(\frac{\lambda\text{range}(\boldsymbol{\beta})}{(M-1)\pi d} + \sin\theta_0\right) - \theta_0\right| \quad (10)$$

If $\boldsymbol{\beta}$ lies in $[-\varepsilon, \varepsilon]$ when $\varepsilon \geq 0$, we have $\text{range}(\boldsymbol{\beta}) \in [0, 2\varepsilon]$. In general, $\arcsin(\theta) \approx \theta$ holds true almost everywhere in the domain except at its boundaries close to -1 and 1, and $\arcsin(\theta) \approx \sin(\theta) \approx \theta$ in the interval [-0.5, 0.5]. Then equation (10) becomes

$$\text{PW}_{\text{PDM}} \approx \frac{2\lambda\text{range}(\boldsymbol{\beta})}{(M-1)\pi d} \leq \frac{4\lambda\varepsilon}{(M-1)\pi d} \quad \theta_0 \in [-0.5, 0.5] \quad (11)$$

The peak width of the PDM in Eq.(10) is small as shown in Fig. 1. Then in the case of multiple narrowband sources with different and unknown center frequencies, the PDM could estimate DOAs through the summation of the PDM estimates in a wide frequency range $[\omega_a, \omega_b]$.

$$P_{\text{PDM}}(\theta) = \sum\nolimits_i \frac{1}{\text{range}(\text{ang}(\boldsymbol{w}_i^* \odot \boldsymbol{X}_i))} \quad (12)$$

where $\boldsymbol{w}_i = \left[1, \text{e}^{-\text{j}\omega_i\tau}, ..., \text{e}^{-\text{j}(M-1)\omega_i\tau}\right]^{\text{T}}$ and ω_i ranges from ω_a to ω_b. $\boldsymbol{X}_i$ denotes $\boldsymbol{X}(\omega_i)$. And *ang* represents the phase angle computation.

3.2 Variance

The minimum of Eq.(9) implies the DOA estimation of the PDM. Removing the computation of the absolute value, the problem is confined to finding the zero crossing point of the following equation:

$$f(\theta) = (M-1)\frac{2\pi d}{\lambda}(\sin\theta - \sin\theta_0) + \beta_M(\theta) - \beta_1(\theta)$$

without loss of generality, we drop the coefficient $(M-1)2\pi d/\lambda$. It becomes

$$y(\theta) = \sin\theta - \sin\theta_0 + w(\theta) \quad (13)$$

where $w(\theta) = \frac{\lambda[\beta_M(\theta) - \beta_1(\theta)]}{2\pi d(M-1)}$. It asymptotically follows the Gaussian distribution $N(0, \sigma_w^2)$, where

$$\sigma_w^2 = \frac{\lambda^2}{\rho[2\pi d(M-1)]^2}$$

Note that $\sin\theta$ is a deterministic signal which has little effect on estimating θ_0. Then the problem of finding the peak location of the PDM spectrum is turned to estimating the direct component $\sin\theta_0$ perturbed by Gaussian noise $w(\theta)$. Its Cramer-Rao bound (CRB) (Kay, 1993) is σ_w^2/L, where L is the number of searching angle in the angle interval defined in Eq.(8). After variable transform, we obtain

$$\text{Var}(\hat{\theta}) = \frac{\lambda^2}{[2\pi d(M-1)]^2(1-\sin^2\theta_0)\rho L} \quad (14)$$

Note that Eq.(14) holds true under the condition of inequality (8). Then we simplify Eq.(14) to the following form (see Appendix B):

$$\text{Var}(\hat{\theta}) \approx \frac{\lambda\Delta\theta}{4\pi^2 d\rho(M-1)(1-\sin^2\theta_0)} \qquad \theta_0 \in [-0.5, 0.5]$$

$$\text{Var}(\hat{\theta}) \geq \frac{\lambda^2\Delta\theta}{\rho[2\pi d(M-1)]^2(1-\sin^2\theta_0)\left[\frac{\pi}{2} - a\sin\left[1 - \frac{\lambda}{(M-1)d}\right]\right]}$$

$$\theta_0 \notin [-0.5, 0.5]$$

where $\Delta\theta$ denotes the angle searching interval. Note that in the discussions above we suppose ω_0 is settled at an integral frequency bin. Therefore, K affects the performance of the PDM through the spectrum leakage.

4 Numerical simulations

Numerical simulations are presented in this section to verify the performance of the PDM compared with that of the CBF method. Of all examples, a 10 elements ULA with K =100 is applied, in which $f_d = c/(2d)$ is the up limit of the frequency to be processed. And the frequency interval $\Delta f = f_s/K$, where f_s is the sample frequency. We take monochromatic signal as the narrowband source. The noise follows the Gaussian distribution $N(0, \sigma^2)$. The SNR is defined as the ratio between the sum of the source power and the noise power.

In the case of single source, Fig.3 presents the peak width of the PDM under different ε after 500 independent trials. Here, a narrowband source with $f_0 = f_d$ emits from $\theta_0 = 0^0$. We add phase interference $\boldsymbol{\beta}$ whose elements

follow the uniform distribution in $[-\varepsilon,\varepsilon]$ to the sensor output spectrum. In Fig.3(a), the curve of Eq.(10) and (11) are overlapped when θ_0=0° And the simulation results are consistent with them. When θ_0=57°≈1, Eq.(10) is still in effect as shown in Fig. 3(b). The root mean square error (RMSE) of the PDM and CBF method compared with the CRB is plotted in Fig.4. Here, both of the PDM and CBF are carried out at ω_0. The RMSE of the CBF is consistent with the CRB curve. However, the RMSE of the PDM could not approach to the CRB due to the loss of the amplitude information.

In the case of multiple narrowband sources with different and unknown center frequencies, we take the PDM estimator defined in Eq.(12). After taking the same operation with the CBF method, the spatial spectra are plotted in Fig.5 when SNR=10dB. Here, four equal power sources with f_0=[0.71, 0.875, 0.94, 1]f_d Hz impinge on the array from θ_0=[−5°, 0°, 10°, 20°]. The PDM distinguishes four sources clearly.

The resolution probability, as shown in Fig.6 after 500 independent trials, is defined as the percentage of simultaneously detecting two sources within an interval of ±0.5° around the actual bearings. In Fig.6(a), the resolution probability in different SNR is presented. Whereas the resolution probability along with different $\Delta\theta$ is shown in Fig.6(b). Apparently, the PDM has better performance than that of the CBF in the case of multiple sources with different center frequencies.

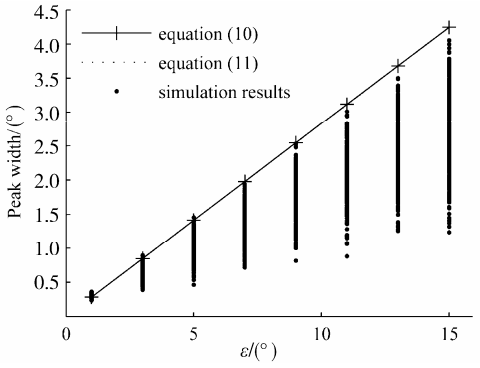

(a) θ_0=0°

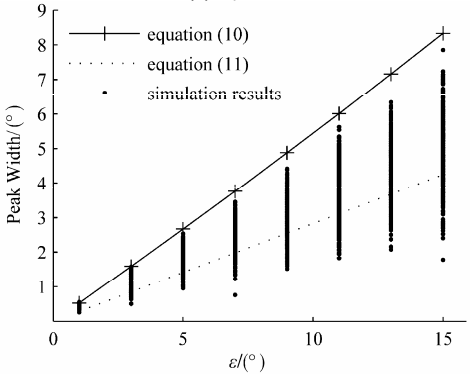

(b) θ_0=57°

Fig. 3 Peak width of the PDM spectrum

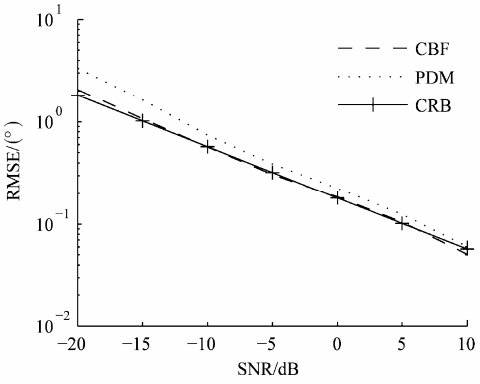

Fig. 4 RMSE of the PDM when θ_0=0°

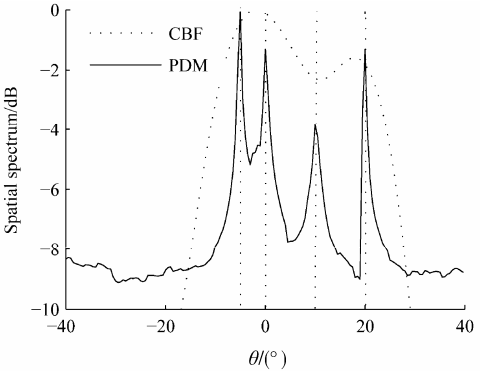

Fig.5 Spatial spectra in the case of four equal power sources

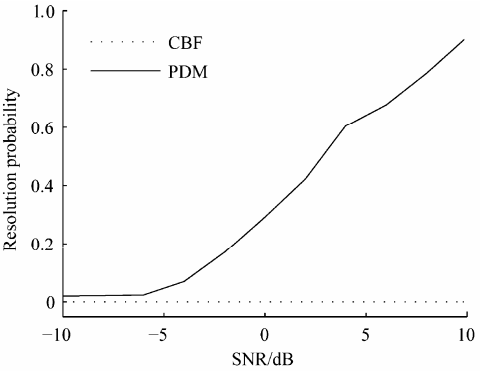

(a) $f_0=[f_d-\Delta f, f_d]$ Hz, θ_0=[0°, 5°] with different SNR

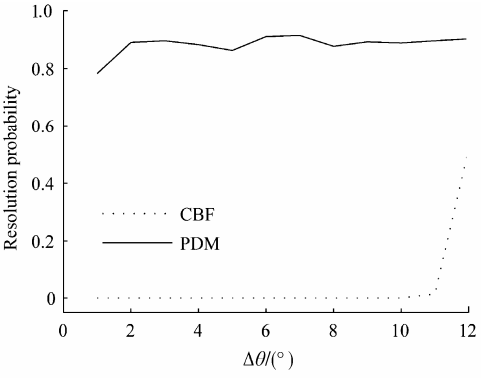

(b) SNR=5dB, $f_0=[f_d-\Delta f, f_d]$ Hz, $\theta_0=[-\Delta\theta/2, \Delta\theta/2]$ with different $\Delta\theta$

Fig. 6 Resolution probability of the PDM

5 Conclusions

The phase difference method for the DOA estimation is introduced. Its peak width and variance are derived. Although the RMSE of the presented method could not approach to the CRB, the PDM can distinguish closely spaced sources with different and unknown center frequencies as long as they are separated with at least one frequency bin.

Appendix A

Proof of $(\beta_M - \beta_1)$ asymptotically follows the Gaussian distribution $N(0,\rho^{-1})$: According to Pawula's results (Pawula, 2001, Pawul *et al.*, 1982), the probability density function (PDF) of the phase difference $(\beta_M - \beta_1)$ is

$$p(\psi) = \frac{1}{2\pi}\int_0^{\pi/2} \exp[-\rho(1-\cos\psi\cos\theta)]\bullet$$
$$(1+\rho+\rho\cos\psi\cos\theta)\cos\theta \mathrm{d}\theta \qquad \text{(A1)}$$

For convenient, we fit Eq.(A1) to the following Gaussian form under 95% confidence interval:

$$p(\psi) = a(\rho)\exp\left\{-\left(\frac{\psi}{b(\rho)}\right)^2\right\}$$

where $a(\rho)$ and $b(\rho)$ are functions of SNR. Next, we carry out the curve fitting between ρ and $a(\rho)$, $b(\rho)$ with the following power form under 95% confidence interval:

$$p(\rho) = c\rho^d$$

Finally, we get

$$p(\psi) \approx 0.3934\rho^{0.5022}\exp\left\{-\left(\frac{\psi}{1.366\rho^{-0.4822}}\right)^2\right\}$$

Defining $\sigma_p = 0.9659\rho^{-0.4822}$, we have

$$p(\psi) = 0.9525\rho^{0.02}\frac{1}{(2\pi\sigma_p^2)^{1/2}}\exp\left\{-\frac{\psi^2}{2\sigma_p^2}\right\}$$

Above 0dB, $\sigma_p \approx \rho^{-0.5}$ and $0.9525\rho^{0.02}$ tend to one. Therefore, $p(\psi)$ approximately follows Gaussian distribution $N(0,\rho^{-1})$ above 0 dB. The Pawula's results are plotted in Fig.7 compared with the fitted Gaussian PDF. They get closer to each other along with the SNR increasing. And the curve of the Gaussian distribution $N(0,\rho^{-1})$ is almost equal to that of Eq.(A1) above 10dB. Then the proposition is proven.

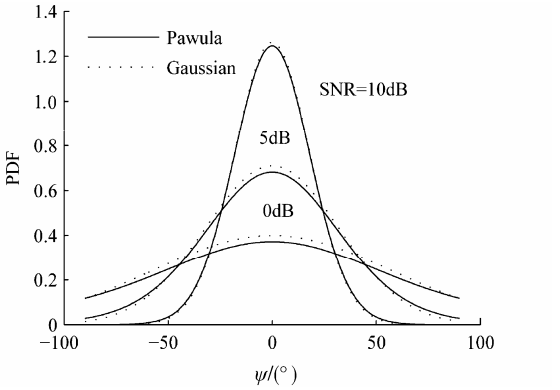

Fig. 7 Phase difference distribution

Appendix B

Simplify Eq.(14): From Eq.(8) we have

$$L = \frac{\arcsin\left[\frac{\lambda(\pi-\alpha)}{(M-1)2\pi d}+\sin\theta_0\right] - \arcsin\left[\frac{-\lambda(\pi+\alpha)}{(M-1)2\pi d}+\sin\theta_0\right]}{\Delta\theta}$$

When $\theta_0 \in [-0.5, 0.5]$, $\mathrm{asin}(\theta) \approx \theta$, it roughly has the following form:

$$L \approx \frac{\lambda}{(M-1)d\Delta\theta} \qquad \theta_0 \in [-0.5, 0.5]$$

Substituting it into Eq.(14), we find

$$\mathrm{Var}(\hat{\theta}) \approx \frac{\lambda\Delta\theta}{4\pi^2 d\rho(M-1)(1-\sin^2\theta_0)}$$
$$\theta_0 \in [-0.5, 0.5] \qquad \text{(A2)}$$

If θ_0 is larger than 0.5, we have

$$\arcsin\left[\frac{\lambda(\pi-\alpha)}{(M-1)2\pi d}+\sin\theta_0\right] \le \frac{\pi}{2}$$

Consequently, it follows that

$$\arcsin\left[\frac{-\lambda(\pi+\alpha)}{(M-1)2\pi d}+\sin\theta_0\right] =$$
$$\arcsin\left[\frac{\lambda(\pi-\alpha)}{(M-1)2\pi d}+\sin\theta_0-\frac{\lambda}{(M-1)d}\right] \ge$$
$$\arcsin\left[1-\frac{\lambda}{(M-1)d}\right]$$

Then L becomes

$$L \le \frac{\frac{\pi}{2}-\arcsin\left[1-\frac{\lambda}{(M-1)d}\right]}{\Delta\theta} \qquad \theta_0 \in \left(0.5, \frac{\pi}{2}\right]$$

Similarly, we have the same result in the interval $[-\pi/2, 0.5)$.

Therefore, we obtain

$$\mathrm{Var}(\hat{\theta}) \geq \frac{\lambda^2 \Delta\theta}{\rho\left[2\pi d(M-1)\right]^2 (1-\sin^2\theta_0)\left[\frac{\pi}{2} - \arcsin\left[1-\frac{\lambda}{(M-1)d}\right]\right]} \quad \theta_0 \notin [-0.5, 0.5] \qquad \text{(A3)}$$

Then Eq.(14) is simplified to (A2) and (A3).

References

Bird JS, Mullins GK (2005). Analysis of swath bathymetry sonar accuracy. *IEEE Journal of Oceanic Engineering*, **30**(2), 372-390.

Carter GC (1987). Coherence and time delay estimation. *Proceedings of the IEEE*, **75**(2), 236-255.

Daeyoung K, Narasimha MJ, Cox DC (1996). An improved single frequency estimator. *IEEE Signal Processing Letters*, **3**(7), 212-214.

Fowler ML (2002). Phase-based frequency estimation: a review. Digital Signal Processing, **12**(4), 590-615.

Fowler ML, Johnson JA (1999). Extending the threshold and frequency range for phase-based frequency estimation. *IEEE Transactions on Signal Processing*, **47**(10), 2857-2863.

Hobiger T, Sekido M, Koyama Y, Kondo T (2009). Integer phase ambiguity estimation in next-generation geodetic very long baseline interferometry. *Advances in Space Research*, **43**(1), 187-192.

Jin W (2008). Modification of frequency estimation algorithms for sinusoidal signals based on phase difference of overlap FFT. *International Conference on Communications, Circuits and Systems*, 927-929.

Kay SM (1989). A fast and accurate single frequency estimator. *IEEE Transactions on Acoustics, Speech, and Signal Processing*, **37**(12), 1987-1990.

Kay SM (1993). *Fundamentals of statistical signal processing: estimation theory*. Prentice-Hall, New Jersey, USA.

Lurton X (2000). Swath bathymetry using phase difference: theoretical analysis of acoustical measurement precision. *IEEE Journal of Oceanic Engineering*, **25**(3), 351-363.

Pawula RF (2001). Distribution of the phase angle between two vectors perturbed by Gaussian noise II. *IEEE Transactions on Vehicular Technology*, **50**(2), 576-583.

Pawula RF, Rice SO, Roberts JH (1982). Distribution of the phase angle between two vectors perturbed by Gaussian noise. *IEEE Transactions on Communications*, **30**(8), 1828-1841.

Shieh CS, Lin CT (2000). Direction of arrival estimation based on phase differences using neural fuzzy network. *IEEE Transactions on Antennas and Propagation*, **48**(7), 1115-1124.

Umesh S, Nelson D (1996). Computationally efficient estimation of sinusoidal frequency at low SNR. *IEEE International Conference on Acoustics, Speech, and Signal Processing*, Atlanta, Georgia, 2797-2800.

Xiao YC, Wei P, Tai HM (2007). Autocorrelation-based algorithm for single-frequency estimation. *Signal Processing*, **87**(6), 1224-1233.

Zhi-fei Chen was born in 1982. He is a PhD student at Northwestern Polytechnical University. His research interests are array signal processing and noise source identification.

Jin-cai Sun was born in 1938. He is a professor at Northwestern Polytechnical University. His research interests include sound signal processing and acoustics.

Hong Hou was born in 1966. He is a professor at Northwestern Polytechnical University. His research interests are acoustics, noise and vibration control.